

Sampling strategies and post-processing methods for OA measurement

R. L. Modini and
S. Takahama

This discussion paper is/has been under review for the journal Atmospheric Measurement Techniques (AMT). Please refer to the corresponding final paper in AMT if available.

Sampling strategies and post-processing methods for increasing the time resolution of organic aerosol measurements requiring long sample collection times

R. L. Modini and S. Takahama

ENAC/IIE Swiss Federal Institute of Technology Lausanne (EPFL), Lausanne, Switzerland

Received: 30 October 2015 – Accepted: 13 December 2015 – Published: 14 January 2016

Correspondence to: S. Takahama (satoshi.takahama@epfl.ch)

Published by Copernicus Publications on behalf of the European Geosciences Union.

Title Page

Abstract

Introduction

Conclusions

References

Tables

Figures

◀

▶

◀

▶

Back

Close

Full Screen / Esc

Printer-friendly Version

Interactive Discussion



Abstract

The composition and properties of atmospheric Organic Aerosols (OAs) change on timescales of minutes to hours. However, some important OA characterization techniques typically require greater than a few hours of sample collection time (e.g. Fourier Transform Infrared (FTIR) spectroscopy). In this study we have performed numerical modeling to investigate and compare sample collection strategies and post-processing methods for increasing the time resolution of OA measurements requiring long sample collection times. Specifically, we modeled the measurement of Hydrocarbon-like OA (HOA) and Oxygenated OA (OOA) concentrations at a polluted urban site in Mexico City, and investigated how to construct hourly-resolved time series from samples collected for 4, 6, and 8 h. We modeled two sampling strategies – sequential and staggered sampling – and a range of post-processing methods including interpolation and deconvolution. The results indicated that relative to the more sophisticated and costly staggered sampling methods, linear interpolation between sequential measurements is a surprisingly effective method for increasing time resolution. Additional error can be added to a time series constructed in this manner if a suboptimal sequential sampling schedule is chosen. Staggering measurements is one way to avoid this effect. There is little to be gained from deconvolving staggered measurements, except at very low values of random measurement error ($< 5\%$). Assuming 20% random measurement error, one can expect average recovery errors of $1.33\text{--}2.81\ \mu\text{g m}^{-3}$ when using 4–8 h long sequential and staggered samples to measure time series of concentration values ranging from $0.13\text{--}29.16\ \mu\text{g m}^{-3}$. For 4 h samples, 19–47% of this total error can be attributed to the process of increasing time resolution alone, depending on the method used, meaning that measurement precision would only be improved by $0.30\text{--}0.75\ \mu\text{g m}^{-3}$ if samples could be collected over 1 h instead of 4 h. Devising a suitable sampling strategy and post-processing method is a good approach for increasing the time resolution of measurements requiring long sample collection times.

Sampling strategies and post-processing methods for OA measurement

R. L. Modini and
S. Takahama

Title Page

Abstract

Introduction

Conclusions

References

Tables

Figures

◀

▶

◀

▶

Back

Close

Full Screen / Esc

Printer-friendly Version

Interactive Discussion



1 Introduction

Organic Aerosols (OAs) comprise 20–90% of total, dry, sub-micrometer atmospheric aerosol mass, and therefore have important influences on air quality and aerosol-climate effects (Jimenez et al., 2009; Fuzzi et al., 2015). OAs can be emitted directly into the atmosphere (Primary Organic Aerosol, POA), or formed in the atmosphere from the oxidation products of precursor gases (Secondary Organic Aerosol, SOA). It is critical to distinguish between POA and SOA since they result from different (natural and anthropogenic) emission and transformation processes, and therefore require separate control and regulation strategies. This separation is complicated by the fact that OAs are complex mixtures of thousands of different individual organic compounds.

A key feature of OA is that its composition and properties change and evolve continually in time (Jimenez et al., 2009). These changes happen on timescales of minutes to hours. OA evolution occurs because organic compounds are subject to continual oxidation throughout their lifetime in the atmosphere, while also mixing with freshly emitted OA. Oxidation changes basic OA molecular properties such as size and degree and type of functionalization. These basic molecular properties determine OA volatility, solubility and hygroscopicity, which in turn determine OA concentrations and the ability of OA to take up water. These effects combined are relevant for assessing aerosol impacts on health and climate. Observation of OA composition over time also permits source resolution important for identifying major contributors to the OA burden in the atmosphere (Corrigan et al., 2013). To capture the evolution of OA composition and properties in the atmosphere it is necessary to measure OA at high time resolution (Jimenez et al., 2009). We define time resolution here as the number of measured values per unit time.

Due to their complexity OAs cannot be completely characterized by any single measurement technique. The full OA picture can only be captured by combining a range of different measurement techniques. Depending on analytical detection limits, some techniques require long sample collection times (typically greater than a few hours) to

Sampling strategies and post-processing methods for OA measurement

R. L. Modini and
S. Takahama

Title Page

Abstract

Introduction

Conclusions

References

Tables

Figures

◀

▶

◀

▶

Back

Close

Full Screen / Esc

Printer-friendly Version

Interactive Discussion



Sampling strategies and post-processing methods for OA measurement

R. L. Modini and
S. Takahama

5 termination of the previous measurement. The time resolution of a sequentially measured time series can be controlled (and increased) by interpolating between measurements. The resolution of a time series obtained by staggered sampling can be controlled through the choice of the staggering interval between samples. A time series resulting from staggered sampling is a running average of the true time series one seeks to measure. In the ideal case, mathematical deconvolution can be used to retrieve the original time series at the resolution of the staggering rather than sample collection interval. For actual measurements, the process of deconvolution is complicated by unavoidable perturbations to measurement signals due to random measurement errors. Regularization techniques are required.

10 We examined two concentration time series with contrasting diurnal patterns. Hydrocarbon-like organic aerosol (HOA) and oxygenated organic aerosol (OOA) are major contributors to OA as identified by AMS and factor analytic decomposition (Zhang et al., 2011). HOA is generally associated with primary organic aerosol (POA) emissions and follows diurnal trends of traffic patterns in urban areas (i.e., early morning and late afternoons during weekdays). OOA is associated with SOA formed from photochemical oxidation in combination with aged background aerosol (de Gouw et al., 2009), and exhibits a peak close to solar noon. The data set we used are AMS measurements of HOA and OOA reported by Aiken et al. (2009) at a polluted urban site in Mexico City, Mexico (T0 site MILAGRO field campaign; Molina et al., 2010). The data set is described fully in Sect. 2.

15 Section 3 formerly introduces and describes the different sampling strategies and post-processing methods we investigated. Section 4 describes the numerical modeling used to apply these sampling strategies and post-processing methods to the test data. The modeled conditions were designed primarily to represent the measurement of functional groups representing HOA and OOA by aerosol FTIR spectroscopy, since this is the primary measurement technique of our research group. However, the results should be applicable to any type of environmental sampling that can be characterized with parameters falling within the ranges that we modeled.

[Title Page](#)[Abstract](#)[Introduction](#)[Conclusions](#)[References](#)[Tables](#)[Figures](#)[◀](#)[▶](#)[◀](#)[▶](#)[Back](#)[Close](#)[Full Screen / Esc](#)[Printer-friendly Version](#)[Interactive Discussion](#)

ods: step function interpolation (Fig. 3a), and linear interpolation (Fig. 3b). Although it seems likely that linear interpolation will better represent the original time series we have tested step interpolation as this case is often assumed (at least implicitly). For both interpolation cases we represented a single measurement by the midpoint of a given sample: each measurement occurs at time $t_{\text{mid}} = t_{\text{start}} + \Delta\tau/2 = t_{\text{end}} - \Delta\tau/2$. It is also possible to represent individual measurements by the start (t_{start}) or endpoints (t_{end}) of each sample. We do not consider those options here because the modeled results do not represent the original time series as well as the simulations with t_{mid} .

3.2 Staggered sampling

Aerosol sample collection can also be staggered, such that each new sample is regularly initiated before termination of the previous sample. By separating successive measurements by a staggering interval $\delta\tau$ less than the individual sample collection time $\Delta\tau$, it is possible to increase measurement time resolution. The principle of combining multiple, overlapping, lower-resolution samples in order to construct higher spatial- and temporal-resolution information has been used extensively for image processing (Borman and Stevenson, 1998; Shechtman et al., 2005).

Staggered sampling effectively applies a running average to a time series of aerosol concentrations, which produces a smeared version of the original signal, denoted here as $g(t)$. If $f(t)$ represents the true change in aerosol concentrations at some point in the atmosphere from time $t = 0$ to T , $g(t)$ is the product of the convolution of a boxcar kernel function $h(\Delta\tau)$ and $f(t)$. This is a specific example of a Fredholm integral equation of the first kind:

$$g(t) = \int_0^T h(\Delta\tau)f(t)dt. \quad (1)$$

In the case of measured data a smeared signal is more appropriately represented by a finite series of n measurement points \mathbf{g} separated by $\delta\tau$ than by the continuous

Sampling strategies and post-processing methods for OA measurement

R. L. Modini and
S. Takahama

Title Page

Abstract

Introduction

Conclusions

References

Tables

Figures

◀

▶

◀

▶

Back

Close

Full Screen / Esc

Printer-friendly Version

Interactive Discussion



function $g(t)$. In addition, all measurements are subject to some amount of measurement uncertainty ϵ . A discrete formulation of Eq. (1) that more accurately reflects the actual measurement process is the matrix equation:

$$\mathbf{g} = \mathbf{H}\mathbf{f} + \epsilon, \quad (2)$$

where \mathbf{H} is a convolution matrix and \mathbf{f} is a finite series of m data points representing $f(t)$. The temporal resolution of \mathbf{f} is $\delta\tau$, the temporal resolution of \mathbf{g} . For staggered samples, the convolution matrix \mathbf{H} is an n -by- m toeplitz matrix. Each of the n rows of \mathbf{H} contains a shifted copy of a boxcar function with $k = \Delta\tau/\delta\tau$ non-zero values equal to $1/k$. In general, $n = m + k - 1$. Figure 5 displays examples of a true time series \mathbf{f} of HOA concentrations and corresponding smeared time series without (Fig. 5a) and with (Fig. 5c) measurement error.

Equation (2) suggests two post-processing methods for recovering a higher time resolution estimate $\hat{\mathbf{f}}$ of the true time series \mathbf{f} from staggered measurements:

1. The measured time series is taken as an approximation of the true time series. No further data processing is applied.
2. One attempts to recover $\hat{\mathbf{f}}$ through a deconvolution operation. For example, if \mathbf{H}^+ is the pseudo-inverse matrix of \mathbf{H} one can solve the following inverse problem

$$\hat{\mathbf{f}} = \mathbf{H}^+\mathbf{g}. \quad (3)$$

In principle, the true aerosol concentrations \mathbf{f} can be recovered precisely from a set of staggered measurements \mathbf{g} and solution of Eq. (3) (Fig. 5b). However, in practice the problem is ill-posed. The small perturbations ϵ to \mathbf{g} due to random measurement uncertainty are strongly amplified in $\hat{\mathbf{f}}$. One can only ever hope to find a solution $\hat{\mathbf{f}}$ that is a good approximation of \mathbf{f} (Fig. 5d and e).

A variety of different deconvolution methods exist for finding the inverse solution of Eq. (2). For example, the convolution theorem (Arfken and Weber, 2005) states that

Sampling strategies and post-processing methods for OA measurement

R. L. Modini and
S. Takahama

Title Page

Abstract

Introduction

Conclusions

References

Tables

Figures

◀

▶

◀

▶

Back

Close

Full Screen / Esc

Printer-friendly Version

Interactive Discussion



correspond to the largest singular values σ_i , and simply discarding the rest. Tikhonov regularization is another common regularization method (Tikhonov and Arsenin, 1977). It involves minimizing a weighted sum of the residual and solution norms, with weighting parameter λ determining the importance given to the solution norm, or smoothness of the solution. The pseudo-inverse matrix is then defined by each method as (Aster et al., 2012)

$$\begin{aligned} \mathbf{H}^+ &= \mathbf{V}_k \mathbf{S}_k^{-1} \mathbf{U}_k^T && \text{TSVD} \\ \mathbf{H}^+ &= (\mathbf{H}^T \mathbf{H} + \lambda \mathbf{I})^{-1} \mathbf{H}^T && \text{Tikhonov,} \end{aligned} \quad (5)$$

where the subscript k indicates the number of components retained, and \mathbf{I} is the identity matrix. As with TSVD, the effect of Tikhonov regularization is to favor the large singular values and deemphasize small singular values. It can be seen that both regularization methods require the introduction and setting of an additional parameter: k for TSVD and λ for Tikhonov regularization. Figure 5d and e illustrate how critical it is to set the regularization parameter to an appropriate value. If too many singular values are retained (large k) or emphasized (small λ) the solution is highly unstable with strongly amplified perturbations. If too few singular values are retained (small k) or emphasized (large λ) the solution is overly smoothed.

4 Description of the modeling

Numerical inverse modeling was conducted with the two test time series to compare the different methods of increasing time resolution (Fig. 2). Table 1 lists the model parameters and their values. The model parameters and values were chosen primarily to represent aerosol sampling for FTIR spectroscopy as detailed further below. However, the calculations are more general, and the results of the numerical modeling are applicable to any type of environmental sampling that can be characterized by parameters falling within the ranges indicated in Table 1.

Sampling strategies and post-processing methods for OA measurement

R. L. Modini and
S. Takahama

Title Page

Abstract

Introduction

Conclusions

References

Tables

Figures

◀

▶

◀

▶

Back

Close

Full Screen / Esc

Printer-friendly Version

Interactive Discussion



Sampling strategies and post-processing methods for OA measurement

R. L. Modini and
S. Takahama

Title Page

Abstract

Introduction

Conclusions

References

Tables

Figures

◀

▶

◀

▶

Back

Close

Full Screen / Esc

Printer-friendly Version

Interactive Discussion



We considered filter sample lengths of 4, 6, and 8 h. A minimum sample length of 4 h represents a typical value for the shortest possible sampling period required for aerosol FTIR spectroscopy (assuming the aerosol is not concentrated before sampling; if the sample is concentrated, FTIR sample collection time can be as short as 1 h, Maria et al., 2002). Sequential sampling was modeled by averaging the true aerosol concentrations over sequential intervals of $\Delta\tau$ hours (e.g. circle markers in Fig. 3) centered at the sample midpoints. Staggered sampling with a staggering interval $\delta\tau$ of 1 h was simulated by constructing a convolution matrix \mathbf{H} (which depends on $\Delta\tau$) and evaluating Eq. (2).

The period of the time series (T) measured by sequential and staggered sampling was varied from 12 to 228 h. To ensure that the same, full, 228 h long HOA and OOA time series were used for each value of T , multiple time series segments were modeled for each $T < 228$ h, and the results are reported as averages over these multiple segments. For example, for $T = 12$ h, 19 ($= 228/12$) separate time series segments were modeled. For $T = 228$ h only a single HOA and a single OOA input time series were required.

Initial testing indicated that the start time of a series of sequential samples affected the ability of the resulting measurement signal to represent the true aerosol concentrations. For example, if a long filter sample is initiated at the apex of a sharp peak in concentration, the resulting measurement does not represent the true changes in aerosol concentrations well. This does not occur for staggered filter samples since more than one sample is collected during a sharp peak (assuming $\delta\tau < \text{peak width}$, which is the case for our test data). Therefore, multiple sequential time series but only a single staggered time series were generated for each modeling run. For example for $\Delta\tau = 4$ h, 4 unique sequential sampling schedules were possible as defined by the following filter start times: [..., 04:00, 08:00, ...], [..., 05:00, 09:00, ...], [..., 06:00, 10:00, ...], and [..., 07:00, 11:00, ...]. For $\Delta\tau = 6$ h, 6 unique sequential sampling schedules were possible, and for $\Delta\tau = 8$ h, 8 unique schedules were possible.

Sampling strategies and post-processing methods for OA measurement

R. L. Modini and
S. Takahama

Title Page

Abstract

Introduction

Conclusions

References

Tables

Figures

◀

▶

◀

▶

Back

Close

Full Screen / Esc

Printer-friendly Version

Interactive Discussion



For both the sequential and staggered cases perturbations due to random measurement error (ϵ , see Eq. 2) were added to the simulated measurements. Relative measurement errors (κ_m) of 0, 1, 5, 10, 20 and 30 % were considered. A relative measurement error of 20 % is typical for aerosol FTIR spectroscopy (Russell, 2003). The relative errors were applied to aerosol mass, not concentration, since this is the quantity actually probed by FTIR spectroscopy (we use the subscript m to denote mass units). A sampling flow rate of 10 lpm was multiplied by the given sampling intervals $\Delta\tau$ to calculate the sampling volumes used to convert between mass and concentration. We assumed that the relative error in the measurement of sampling flow rate was 2 %. The relative error in the measurement of the sampling time interval $\Delta\tau$ was assumed to be so small in comparison to the errors in measured mass and flow rate that it could be neglected. The relative uncertainties in measured mass and flow rate were summed in quadrature to calculate total, relative uncertainty in aerosol concentration, denoted as κ_c , where the subscript c indicates concentration units.

The relative error was combined with a fixed error term ($\sigma_{0,m}$). The fixed error term represents, for example, the standard deviation of masses detectable on blank filter samples. The fixed error term is typically on the order of 0.1 μg for aerosol FTIR samples on Teflon filters. We conservatively set $\sigma_{0,m}$ to 0.5 μg , which is at the upper end of the range of blank uncertainty values measured in previous FTIR studies (Maria et al., 2003; Gilardoni et al., 2009, 2007). A fixed error of 0.5 μg is consistent with the selected minimum sampling interval of 4 h (Table 1). Defining detection limit as $3\sigma_{0,m}$, 4 h of sampling would be required to ensure that almost all (> 97 %) of the organic functional group samples representing HOA and OOA collected during the time period covered by the test time series were above detection limit (Fig. S1 in the Supplement). We also modeled $\sigma_{0,m} = 0.1 \mu\text{g}$. The results were insensitive to this change so are not included here.

Taking the relative and fixed errors, total measurement error σ as a function of concentration c was calculated with the linear error model described by Eq. (6). Linear dependence of total measurement error on concentration is a widely applicable as-

ing equation

$$UE = RE - ME = RE - \frac{1}{n} \sum_{i=1}^n |f_i - f'_i|, \quad (8)$$

where ME is defined as the mean absolute error between a true time series f consisting of n data points and a time series f' produced by a hypothetical instrument subject to the same random error modeled by our linear error model, but capable of measuring at hourly rather than 4–8 h time resolution. We choose to report the bulk of the results as RE to represent the total error resulting from the upsampling of noisy measurements. In the final discussion Sect. 9 we also report typical UEs to illustrate how much of the total error can be attributed solely to the upsampling process.

2. Peak capture: the specific ability to recover the magnitude and timing of the daily concentration peaks (indicated by the circle markers in Fig. 1). The ability of a method to accurately capture peaks in concentration is important for health and regulatory concerns (e.g. for identifying exceedances of particulate matter air quality guidelines). We assess peak capture through a peak plot, which displays the mean difference between the daily peak concentrations in a calculated hourly-resolved time series and the corresponding peak concentrations in the true time series, against the mean difference between the times that the peaks occur in the calculated time series and in the corresponding true time series.

In the discussion of the modeling results we pay particular attention to the measurements of 57 h long time periods with 4 h samples subject to 20 % measurement error. This represents a typical FTIR experiment. However, the dependence of recovery error on time series period, filter sample length, and the level of measurement error is also discussed.

Sampling strategies and post-processing methods for OA measurement

R. L. Modini and
S. Takahama

Title Page

Abstract

Introduction

Conclusions

References

Tables

Figures

◀

▶

◀

▶

Back

Close

Full Screen / Esc

Printer-friendly Version

Interactive Discussion



5 Sequential sampling results

This section identifies the best representation (step or linear) of atmospheric concentrations using sequential samples and discusses the issue of sequential sampling schedule. These questions are answered with reference to overall recovery error (RE, Sect. 4) since the ability to capture peak concentrations with sequential samples does not depend on the interpolation method employed (unless higher order interpolation functions are used).

Figure 6a–f shows the dependence of RE on the start time of the second sample of the day for HOA and OOA time series that were constructed by step and linear interpolation between sequential samples of sampling length ($\Delta\tau$) 4, 6, and 8 h ($T = 57$ h and $\kappa_m = 20\%$). The start time of the second sample of the day represents sample schedule. For both HOA and OOA, RE is generally lower for the linearly interpolated solutions than the step interpolated solutions, and RE increases with increasing $\Delta\tau$. Figures S2 and S3 in the Supplement indicate that linear interpolation results in lower recovery error than step interpolation over the full ranges of simulated time series periods and relative measurement errors, respectively. Therefore not surprisingly, linear interpolation is a more effective method for post-processing sequential measurement than step interpolation.

Fig. 6g plots the maximum difference in RE between two different sampling schedules (designated as maximum ΔRE) against $\Delta\tau$. Maximum ΔRE can be thought of the extra error that may be incurred if a bad sampling schedule is chosen for a particular type of time series. For $\Delta\tau = 4$ h, RE is relatively independent of the particular sampling schedule employed. Additional error of 0.13 to 0.20 $\mu\text{g m}^{-3}$ is possible if the suboptimal sampling schedule is chosen. This compares with mean REs of 1.49 for HOA and 1.85 $\mu\text{g m}^{-3}$ for OOA time series constructed with linear interpolation. Maximum ΔRE increases with $\Delta\tau$. For $\Delta\tau = 8$ h, additional error of 0.42 to 0.90 $\mu\text{g m}^{-3}$ is possible if the suboptimal sampling schedule is chosen. In comparison mean REs were 1.96 for HOA and 2.51 $\mu\text{g m}^{-3}$ for OOA time series constructed by linear interpolation. Since the op-

Sampling strategies and post-processing methods for OA measurement

R. L. Modini and
S. Takahama

Title Page

Abstract

Introduction

Conclusions

References

Tables

Figures

◀

▶

◀

▶

Back

Close

Full Screen / Esc

Printer-friendly Version

Interactive Discussion



5 timal sequential sampling schedule cannot be known a priori, the additional error that may be incurred due to this scheduling effect must be kept in mind when interpolating between sequential samples, particularly for measurements requiring sample collection times > 6 h. This scheduling effect is not as important for staggered samples, assuming the staggering interval is small enough, since measurement data points are collected more frequently.

6 Deconvolution results

10 Eight different combinations of regularization and boundary value methods (Fig. 2) were used to recover time series by deconvolution for each set of simulated staggered measurements. For $T = 57$ h and $\kappa_m = 20\%$, Fig. 7 displays the mean RE of deconvolution solutions recovered by TSVD and Tikhonov regularization as a function of the boundary value method employed (tiled by $\Delta\tau$ and time series type), and Fig. 8 displays a peak plot for each combination of regularization and boundary value method.

15 At this relatively high level of measurement error, only a small reduction in RE is gained from having access to the full measurement vector (which would require the collection of partial samples, Sect. 3). Furthermore, there is little difference in the mean RE of the 3 methods that assume boundary values are not accessible to measurement: no clear and consistent advantage can be discerned between the truncated, uniformly, and reflectively padded methods for this T and κ_m . Assuming the boundary values are known, the average RE of HOA time series sampled with 4 h filters and recovered with TSVD regularization is $1.16 \mu\text{g m}^{-3}$. If the boundary values are not known, the corresponding value averaged over the three other boundary value methods is $1.34 \mu\text{g m}^{-3}$. The corresponding OOA-TSVD results tell the same story: RE of $1.42 \mu\text{g m}^{-3}$ with the full measurement vector vs. an average of $1.65 \mu\text{g m}^{-3}$ over the 3 methods without. The results are similar over the full range of time series periods simulated (Fig. S4 in the Supplement).

Sampling strategies and post-processing methods for OA measurement

R. L. Modini and
S. Takahama

Title Page

Abstract

Introduction

Conclusions

References

Tables

Figures

◀

▶

◀

▶

Back

Close

Full Screen / Esc

Printer-friendly Version

Interactive Discussion



Sampling strategies and post-processing methods for OA measurement

R. L. Modini and
S. Takahama

Title Page

Abstract

Introduction

Conclusions

References

Tables

Figures

◀

▶

◀

▶

Back

Close

Full Screen / Esc

Printer-friendly Version

Interactive Discussion



context of the practical considerations and limitations of each method. Interpolation between sequential measurements is the least sophisticated, cheapest and easiest of the methods for increasing time resolution out of those that we have investigated. Staggered sampling requires multiple sampling lines to collect multiple samples at once. More staggered samples are required to cover a given time period than would be required to cover the same time period with sequential samples. This extra cost of staggered sampling compared to sequential sampling is illustrated in Fig. 9. For example, to measure a time series of period 64 h, 61 staggered 4 h samples would be required compared to only 16 sequential 4 h samples. The sample number difference is even greater for larger $\Delta\tau$. To measure a time series of period 64 h, 57 staggered 8 h samples would be required compared to only 8 sequential 8 h samples.

Attempting to recover the true time series from a set of staggered measurements by deconvolution requires even further effort and analysis time and expertise. Although tried and tested deconvolution and regularization algorithms are readily available (Hansen, 2007), the choice of a reasonable regularization parameter may not be straightforward. If a bad regularization parameter is chosen substantial additional error could be added to a solution (Fig. 5). Given the extra cost of staggered sampling and the error risk associated with regularization, it is necessary to establish precisely what, if anything, can be gained from the use of these more sophisticated tactics for a variety of different experimental conditions.

Figure 10 displays the mean recovery error as a function of κ_m for HOA and OOA time series processed by the sequential, smeared, and recovered methods ($T = 57$ h and $\Delta\tau = 4$ h). Two sequential cases are displayed. Both were obtained by linear interpolation. “Sequential low” corresponds to the sampling schedule that resulted in the lowest RE, and “sequential high” corresponds to the sampling schedule that resulted in the highest RE. The RE difference between these two cases is the sequential sampling effect identified in Fig. 6g. The recovered solutions were produced by deconvolution with TSVD regularization and the truncated method for dealing with inaccessible boundary values (Sect. 6). As expected, in the absence of measurement error, recov-

Sampling strategies and post-processing methods for OA measurement

R. L. Modini and
S. Takahama

Title Page

Abstract

Introduction

Conclusions

References

Tables

Figures

◀

▶

◀

▶

Back

Close

Full Screen / Esc

Printer-friendly Version

Interactive Discussion



ering a time series through the deconvolution of staggered measurements is the best method for achieving high time resolution. On average, true concentrations can be reproduced to within $0.25 \mu\text{g m}^{-3}$ for HOA and $0.48 \mu\text{g m}^{-3}$ for OOA with this method (RE is not zero because of the truncated measurement vector). However, measurement error is unavoidable, and the presence of only 5% error is sufficient for the recovered method to lose its RE advantage over the less sophisticated sequential and smeared methods.

At the 20% level of relative measurement error characteristic for aerosol FTIR spectroscopy, the differences in mean RE between the optimally-scheduled sequential, smeared, and recovered are very small. For HOA, mean RE is 1.49, 1.39, and $1.33 \mu\text{g m}^{-3}$ for the sequential low, smeared and recovered time series, respectively. However, if a suboptimal sampling schedule is chosen, mean RE for the HOA time series could be as high as $1.58 \mu\text{g m}^{-3}$. In a real experiment there would be no way of knowing what the optimal sequential sampling schedule was (unless a complementary independent measurement was available), and therefore whether a sequentially measured time series would be subject to the higher amount of error or not. Collecting staggered samples is one option for avoiding the sample scheduling effect.

The peak plots corresponding to the REs shown in Fig. 10 for $\kappa_m = 20\%$ are displayed in Fig. 11. Both the optimally- and suboptimally-scheduled sequential solutions are slightly worse at capturing peak concentrations than the smeared and recovered solutions. For example, peak HOA concentrations are underestimated by an average of $4.28 \mu\text{g m}^{-3}$ in the optimally-scheduled sequential solution compared to 3.32 and $2.74 \mu\text{g m}^{-3}$ for the smeared and recovered solutions respectively. For the OOA time series, peak concentration values are reproduced, on average, very accurately in the smeared and recovered solutions, being overpredicted by only 0.85 and $0.43 \mu\text{g m}^{-3}$, respectively. The same peak concentrations are underestimated by $1.94 \mu\text{g m}^{-3}$ in the optimally-scheduled sequential solution.

A key variable included in our numerical model is the filter sample length $\Delta\tau$. Figure 12 displays mean RE against $\Delta\tau$ for the same cases shown in Figs. 10 and 11.

Sampling strategies and post-processing methods for OA measurement

R. L. Modini and
S. Takahama

Title Page

Abstract

Introduction

Conclusions

References

Tables

Figures

◀

▶

◀

▶

Back

Close

Full Screen / Esc

Printer-friendly Version

Interactive Discussion



Again $T = 57$ h and $\kappa_m = 20\%$. It is interesting to note that mean RE does not depend strongly on $\Delta\tau$ for the optimally-scheduled sequential, smeared and recovered cases. For example, if 4 h samples are used to construct an hourly-resolved OOA time series using the smeared method, true concentrations can be reproduced to within an average of $1.81 \mu\text{g m}^{-3}$. If 8 h samples are used to construct the same hourly-resolved time series via the same smeared method, the reproduction error is only slightly greater, $2.15 \mu\text{g m}^{-3}$. However in the case of suboptimally-scheduled sequential measurements the increase in RE with $\Delta\tau$ is considerably greater because the sequential sampling scheduling effect increases with increasing sample collection time (Fig. 6g)

Whether or not the differences between the sequential, smeared and recovered methods are significant depends on the specific aims of a given experiment. If the priority is to achieve low overall error over long time periods when measuring a concentration time series with 4 h samples subject to 20 % relative measurement error, linear interpolation between sequentially collected samples is likely to be a suitable enough choice for achieving hourly time resolution. Additional error may be inadvertently introduced through choice of a suboptimal sampling schedule but the extra practical costs of staggered sampling (Fig. 9) would be avoided. On the other hand, if one was particularly interested in accurately measuring peak OA concentrations and had the ability to run multiple sampling lines at once, then staggered sampling with no further data processing would be the best option for achieving hourly time resolution (Fig. 11). A combination of sequential sampling during stable OA concentration periods and staggered sampling during peak periods (e.g. morning rush hour, afternoon peak in photochemistry) could be an excellent strategy for intensive field campaigns.

Our analysis suggests that in scenarios similar to the case studied in this work there is little benefit to be gained (in terms of both overall error and peak capture) by running staggered measurements through a deconvolution algorithm. This is surprising given that in the absence of perturbations to a measurement signal, true concentrations can be recovered precisely from a set of staggered measurements (Fig. 5b). However, once non-ideal, practical realities such as random measurement error (even as low as 5 %)

Sampling strategies and post-processing methods for OA measurement

R. L. Modini and
S. Takahama

Title Page

Abstract

Introduction

Conclusions

References

Tables

Figures

◀

▶

◀

▶

Back

Close

Full Screen / Esc

Printer-friendly Version

Interactive Discussion



prisingly, for the case $T = 57$ h and $\Delta\tau = 4$ h, only 19–47% of the overall recovery error can be attributed to the actual upsampling process. In absolute terms, this indicates that measurement precision would only be improved by 0.30–0.75 $\mu\text{g m}^{-3}$ if samples could be collected over 1 h instead of 4 h.

The total and upsampling errors we have reported represent only small fractions of the average daily peak concentrations in the HOA and OOA test time series. Therefore, post-processing methods are effective techniques for increasing the time resolution of OA measurements requiring long sample collection times. Application of these methods should be considered as a good alternative or complement to other methods of achieving high time resolution, such as instrument redesign for rapid sample collection, which in many cases may be prohibitively expensive.

Acknowledgements. The authors thank J. L. Jimenez for providing the aerosol mass spectrometry data, V. M. Panaretos for interesting and informative discussions on inverse problems and the treatment of boundary values, and EPFL for funding. R. L. M. acknowledges support from the “EPFL Fellows” fellowship programme co-funded by Marie Curie, FP7 Grant agreement no. 291771.

References

- Aiken, A. C., Salcedo, D., Cubison, M. J., Huffman, J. A., DeCarlo, P. F., Ulbrich, I. M., Docherty, K. S., Sueper, D., Kimmel, J. R., Worsnop, D. R., Trimborn, A., Northway, M., Stone, E. A., Schauer, J. J., Volkamer, R. M., Fortner, E., de Foy, B., Wang, J., Laskin, A., Shutthanandan, V., Zheng, J., Zhang, R., Gaffney, J., Marley, N. A., Paredes-Miranda, G., Arnott, W. P., Molina, L. T., Sosa, G., and Jimenez, J. L.: Mexico City aerosol analysis during MILAGRO using high resolution aerosol mass spectrometry at the urban supersite (T0) – Part 1: Fine particle composition and organic source apportionment, *Atmos. Chem. Phys.*, 9, 6633–6653, doi:10.5194/acp-9-6633-2009, 2009. 5, 6, 7, 34
- Arfken, G. B. and Weber, H.-J.: *Mathematical Methods for Physicists*, Elsevier, Burlington, MA, USA, 2005. 10

Sampling strategies and post-processing methods for OA measurement

R. L. Modini and
S. Takahama

Title Page

Abstract

Introduction

Conclusions

References

Tables

Figures

◀

▶

◀

▶

Back

Close

Full Screen / Esc

Printer-friendly Version

Interactive Discussion

- Aster, R., Borchers, B., and Thurber, C.: Parameter Estimation and Inverse Problems, Academic Press, Waltham, MA, 2nd edn., 2012. 13
- Borman, S. and Stevenson, R.: Spatial Resolution Enhancement of Low-Resolution Image Sequences – A Comprehensive Review with Directions for Future Research, Department of Electrical Engineering, University of Notre Dame, Notre Dame, Indiana, USA, Tech. rep., 1998. 9
- Calvetti, D., Kaipio, J. P., and Someralo, E.: Aristotelian prior boundary conditions, *Int. J. Math. Comp. Sci.*, 63–81, 2006. 12
- Corrigan, A. L., Russell, L. M., Takahama, S., Äijälä, M., Ehn, M., Junninen, H., Rinne, J., Petäjä, T., Kulmala, M., Vogel, A. L., Hoffmann, T., Ebben, C. J., Geiger, F. M., Chhabra, P., Seinfeld, J. H., Worsnop, D. R., Song, W., Auld, J., and Williams, J.: Biogenic and biomass burning organic aerosol in a boreal forest at Hyytiälä Finland, during HUMPPA-COPEC 2010, *Atmos. Chem. Phys.*, 13, 12233–12256, doi:10.5194/acp-13-12233-2013, 2013. 3, 4, 8
- de Gouw, J. A., Welsh-Bon, D., Warneke, C., Kuster, W. C., Alexander, L., Baker, A. K., Beyersdorf, A. J., Blake, D. R., Canagaratna, M., Celada, A. T., Huey, L. G., Junkermann, W., Onasch, T. B., Salcido, A., Sjostedt, S. J., Sullivan, A. P., Tanner, D. J., Vargas, O., Weber, R. J., Worsnop, D. R., Yu, X. Y., and Zaveri, R.: Emission and chemistry of organic carbon in the gas and aerosol phase at a sub-urban site near Mexico City in March 2006 during the MILAGRO study, *Atmos. Chem. Phys.*, 9, 3425–3442, doi:10.5194/acp-9-3425-2009, 2009. 5
- Decesari, S., Fuzzi, S., Facchini, M. C., Mircea, M., Emblico, L., Cavalli, F., Maenhaut, W., Chi, X., Schkolnik, G., Falkovich, A., Rudich, Y., Claeys, M., Pashynska, V., Vas, G., Kourtchev, I., Vermeylen, R., Hoffer, A., Andreae, M. O., Tagliavini, E., Moretti, F., and Artaxo, P.: Characterization of the organic composition of aerosols from Rondônia Brazil, during the LBA-SMOCC 2002 experiment and its representation through model compounds, *Atmos. Chem. Phys.*, 6, 375–402, doi:10.5194/acp-6-375-2006, 2006. 4
- Ehrlich, A. and Wendisch, M.: Reconstruction of high-resolution time series from slow-response broadband terrestrial irradiance measurements by deconvolution, *Atmos. Meas. Tech.*, 8, 3671–3684, doi:10.5194/amt-8-3671-2015, 2015. 11
- Finessi, E., Decesari, S., Paglione, M., Giulianelli, L., Carbone, C., Gilardoni, S., Fuzzi, S., Saarikoski, S., Raatikainen, T., Hillamo, R., Allan, J., Mentel, T. F., Tiitta, P., Laaksonen, A., Petäjä, T., Kulmala, M., Worsnop, D. R., and Facchini, M. C.: Determination of the biogenic

Sampling strategies and post-processing methods for OA measurement

R. L. Modini and
S. Takahama

Title Page

Abstract

Introduction

Conclusions

References

Tables

Figures

◀

▶

◀

▶

Back

Close

Full Screen / Esc

Printer-friendly Version

Interactive Discussion

born, A. M., Williams, L. R., Wood, E. C., Middlebrook, A. M., Kolb, C. E., Baltensperger, U., and Worsnop, D. R.: Evolution of organic aerosols in the atmosphere, *Science*, 326, 1525–1529, doi:10.1126/science.1180353, 2009. 3

Lane, R. G., Irwan, R., and Bones, P. J.: Effects of truncation on deconvolution, *SPIE Proc. Ser.*, 3171, 64–75, doi:10.1117/12.284711, 1997. 12

Maria, S. F., Russell, L. M., Turpin, B. J., and Porcja, R. J.: FTIR measurements of functional groups and organic mass in aerosol samples over the Caribbean, *Atmos. Environ.*, 36, 5185–5196, doi:10.1016/S1352-2310(02)00654-4, 2002. 4, 14

Maria, S. F., Russell, L. M., Turpin, B. J., Porcja, R. J., Campos, T. L., Weber, R. J., and Huebert, B. J.: Source signatures of carbon monoxide and organic functional groups in Asian Pacific Regional Aerosol Characterization Experiment (ACE-Asia) submicron aerosol types, *J. Geophys. Res.-Atmos.*, 108, 8637, doi:10.1029/2003JD003703, 2003. 15

Matta, E., Facchini, M. C., Decesari, S., Mircea, M., Cavalli, F., Fuzzi, S., Putaud, J.-P., and Dell'Acqua, A.: Mass closure on the chemical species in size-segregated atmospheric aerosol collected in an urban area of the Po Valley Italy, *Atmos. Chem. Phys.*, 3, 623–637, doi:10.5194/acp-3-623-2003, 2003. 4

Molina, L. T., Madronich, S., Gaffney, J. S., Apel, E., de Foy, B., Fast, J., Ferrare, R., Herndon, S., Jimenez, J. L., Lamb, B., Osornio-Vargas, A. R., Russell, P., Schauer, J. J., Stevens, P. S., Volkamer, R., and Zavala, M.: An overview of the MILAGRO 2006 Campaign: Mexico City emissions and their transport and transformation, *Atmos. Chem. Phys.*, 10, 8697–8760, doi:10.5194/acp-10-8697-2010, 2010. 5, 6

Ripley, B. D. and Thompson, M.: Regression techniques for the detection of analytical bias, *Analyst*, 112, 377–383, doi:10.1039/AN9871200377, 1987. 16

Russell, L.: Aerosol organic-mass-to-organic-carbon ratio measurements, *Environ. Sci. Technol.*, 37, 2982–2987, 2003. 15

Russell, L. M., Takahama, S., Liu, S., Hawkins, L. N., Covert, D. S., Quinn, P. K., and Bates, T. S.: Oxygenated fraction and mass of organic aerosol from direct emission and atmospheric processing measured on the R/V Ronald Brown during TEXAQS/GoMACCS 2006, *J. Geophys. Res.-Atmos.*, 114, D00F05, doi:10.1029/2008JD011275, 2009. 7

Russell, L. M., Bahadur, R., and Ziemann, P. J.: Identifying organic aerosol sources by comparing functional group composition in chamber and atmospheric particles, *P. Natl. Acad. Sci. USA*, 108, 3516–3521, doi:10.1073/pnas.1006461108, 2011. 4

Sampling strategies and post-processing methods for OA measurement

R. L. Modini and
S. Takahama

Table 1. Modeling parameters.

| Parameter | Description | Value(s) |
|----------------------------------|---|------------------------------|
| $\Delta\tau$ (h) | Sample collection or measurement integration time | 4, 6, 8 |
| $\delta\tau$ (h) | Staggering interval | 1 |
| T (h) | Period of time series being measured | 12, 19, 38, 57, 76, 114, 228 |
| κ_m (% of mass) | Relative measurement error | 0, 1, 5, 10, 20, 30 |
| $\sigma_{0,m}$ (μg) | Fixed or blank measurement error | 0.5 |

Title Page

Abstract

Introduction

Conclusions

References

Tables

Figures

◀

▶

◀

▶

Back

Close

Full Screen / Esc

Printer-friendly Version

Interactive Discussion



Sampling strategies and post-processing methods for OA measurement

R. L. Modini and
S. Takahama

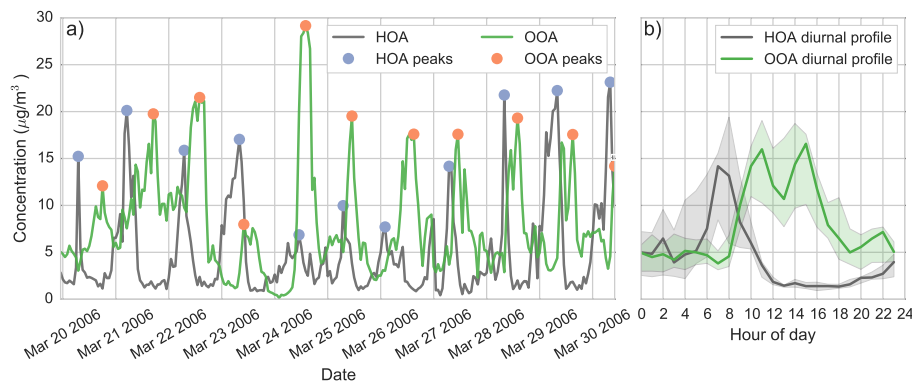


Figure 1. (a) Time series of HOA (dark gray) and OOA (green) concentrations measured at the T0 site in Mexico City during the MILAGRO field campaign (Aiken et al., 2009). Blue and orange circle markers indicate the daily HOA and OOA peaks, respectively, used for the peak reproduction analysis (Sect. 4). (b) Diurnally averaged HOA and OOA concentrations.

Sampling strategies and post-processing methods for OA measurement

R. L. Modini and
S. Takahama

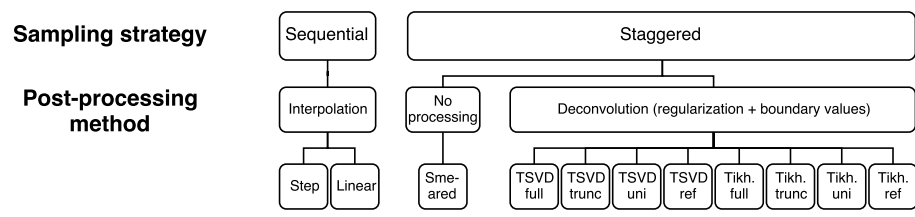


Figure 2. Sampling strategies and post-processing methods for increasing time resolution. Each method is explained in detail in the main text in Sect. 3. Step: step function, linear: linear function, TSVD: TSVD regularization, Tikh.: Tikhonov regularization, full: no loss of the boundary values corresponding to partial measurement samples, trunc: loss of all boundary values corresponding to partial measurement samples, uni: truncated signal uniformly padded to the length of the full, smeared signal, ref: truncated signal reflectively padded to the length of the full, smeared signal.

| | |
|--------------------------|--------------|
| Title Page | |
| Abstract | Introduction |
| Conclusions | References |
| Tables | Figures |
| ◀ | ▶ |
| ◀ | ▶ |
| Back | Close |
| Full Screen / Esc | |
| Printer-friendly Version | |
| Interactive Discussion | |



Sampling strategies and post-processing methods for OA measurement

R. L. Modini and
S. Takahama

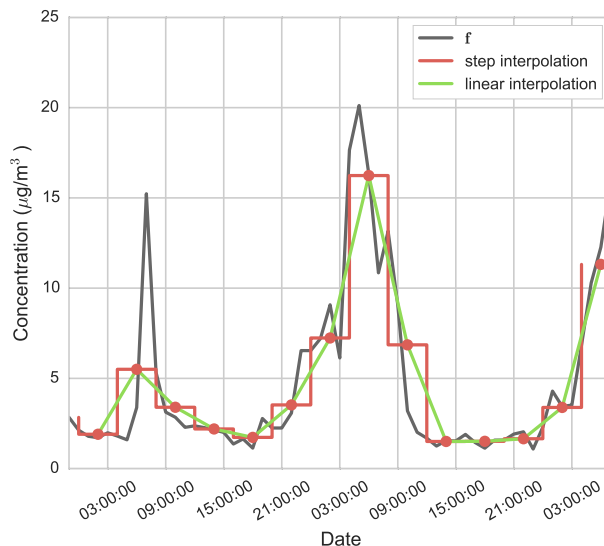


Figure 3. An illustrative example of interpolation between sequential samples. An original time series f of HOA concentrations, and the time series resulting from step (red) and linear (yellow) interpolation between successive sequential samples, which are indicated by the circle markers.

[Title Page](#)[Abstract](#)[Introduction](#)[Conclusions](#)[References](#)[Tables](#)[Figures](#)[◀](#)[▶](#)[◀](#)[▶](#)[Back](#)[Close](#)[Full Screen / Esc](#)[Printer-friendly Version](#)[Interactive Discussion](#)

Sampling strategies and post-processing methods for OA measurement

R. L. Modini and
S. Takahama

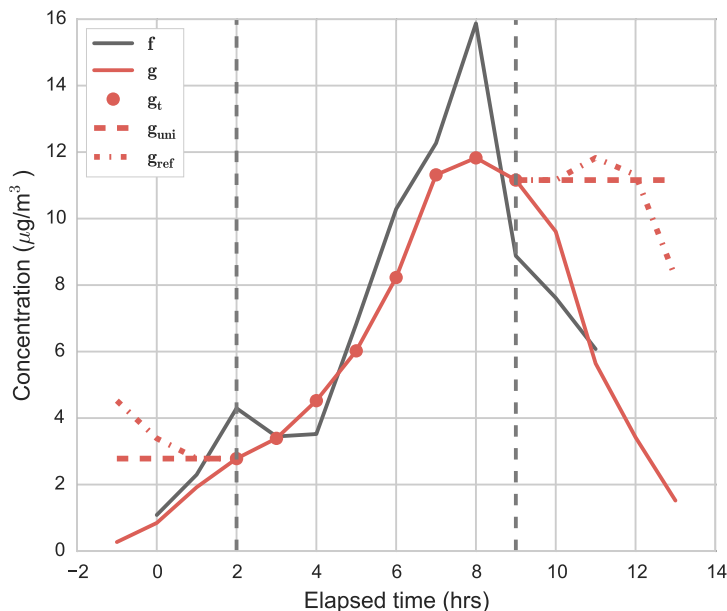


Figure 4. An original time series f of period $T = 12$ h measured with 4 h samples ($\Delta\tau = 4$ h) staggered at intervals of 1 h ($\delta\tau = 1$ h). The resulting smeared signal g is the full convolution product of f and a convolution matrix $\mathbf{H}(\Delta\tau, \delta\tau)$. Since f contains 12 data points, g contains 15 ($= 12 + (4/1) - 1$) data points. The values at the boundaries of g correspond to partial averages of f (samples with sampling time $< \Delta\tau$). In practice these values are often not accessible to measurement, and one is left with a truncated measurement vector g_t consisting of only 8 ($= 15 - 2(4 - 0.5)$) data points. The truncated measurement vector can be padded on its edges by the uniform (g_{uni}) or reflective (g_{ref}) methods so that it has the same number of elements as the full convolution product g .

Sampling strategies and post-processing methods for OA measurement

R. L. Modini and
S. Takahama

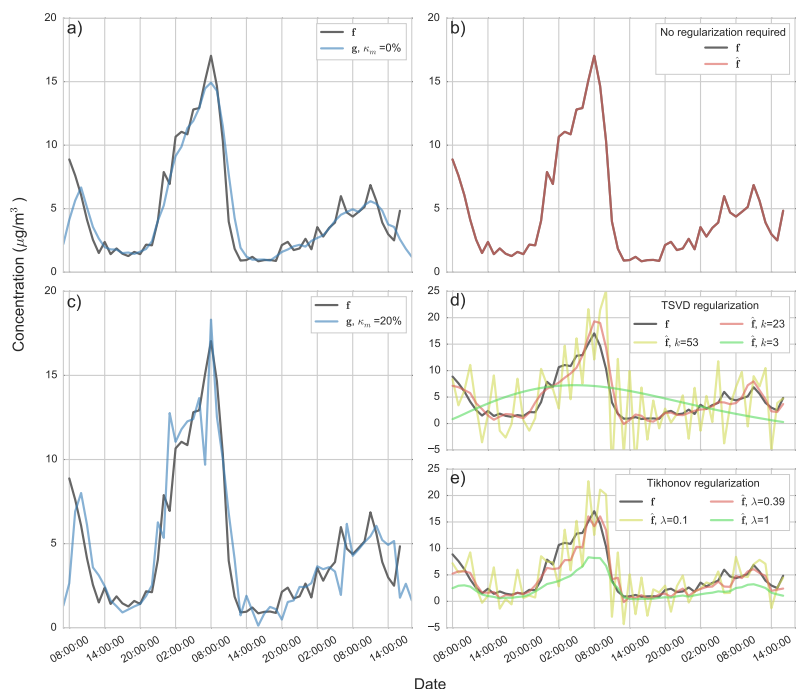


Figure 5. Explanation of different types of time series: f is an original time series of HOA concentrations; g are smeared time series produced from the staggering of 4 h samples ($\Delta\tau = 4$ h) at 1 h intervals ($\delta\tau = 1$ h) (a) without ($\kappa_m = 0\%$) and (c) with the addition of normally-distributed random measurement error ($\kappa_m = 20\%$). The right panels contain time series \hat{f} recovered by deconvolution of the smeared time series g in the corresponding left panels. When $\kappa_m = 0\%$ (b), the true time series can be completely recovered by deconvolution. No regularization is required. When $\kappa_m = 20\%$, (d) TSVD regularization with appropriate choice of k ($= 23$), or (e) Tikhonov regularization with appropriate choice of λ ($= 0.39$) are required to obtain solutions that approximate the true time series well.

Sampling strategies and post-processing methods for OA measurement

R. L. Modini and
S. Takahama

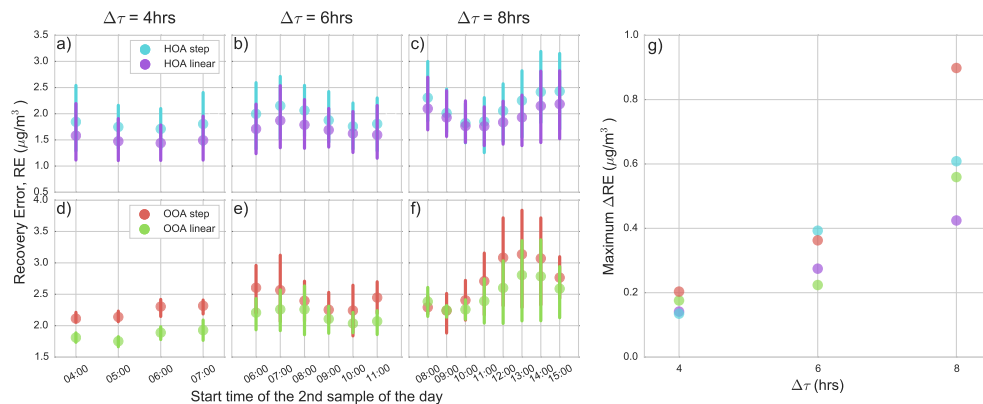


Figure 6. (a–f) Mean Recovery error (RE) as a function of the start time of the second sample of the day for HOA and OOA time series constructed by step and linear interpolation between sequential measurements of length ($\Delta\tau$) 4, 6, and 8 h. $\kappa_m = 20\%$ and $T = 57$ h, meaning each data point is an average over 4 ($= 228/57$) time series segments. The start time of the second sample of the day represents the 4, 6, and 8 unique sequential sampling schedules that are possible with 4, 6, and 8 h samples, respectively (Sect. 4). The vertical bars represent 95 % confidence intervals determined by bootstrapping the mean estimates. (g) Maximum ΔRE vs. $\Delta\tau$. Maximum ΔRE represents the maximum difference in RE between two unique sampling schedules for a given $\Delta\tau$. It is the maximum possible potential error that may be incurred if a suboptimal sampling schedule is chosen for a given type of time series.

Sampling strategies and post-processing methods for OA measurement

R. L. Modini and
S. Takahama

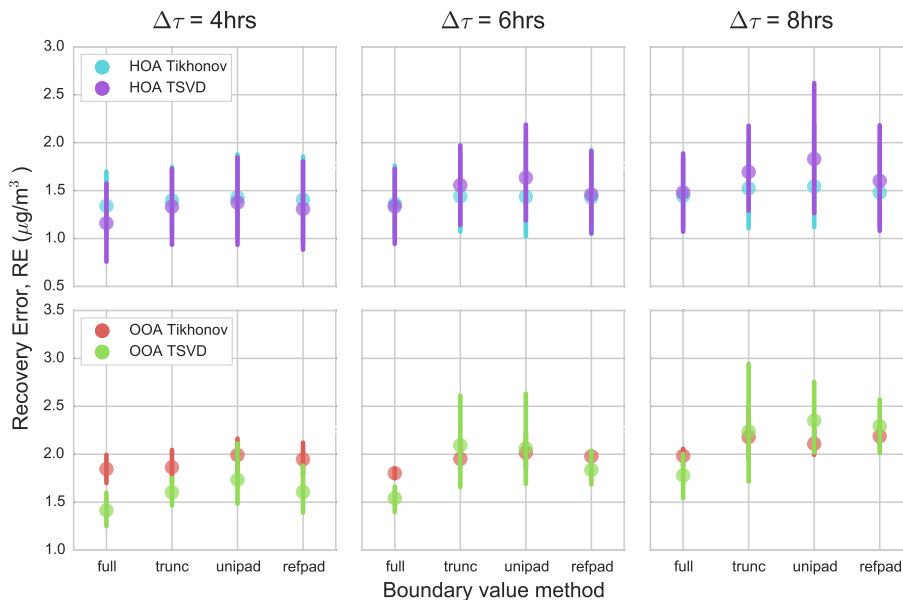


Figure 7. Mean Recovery error (RE) for different boundary value methods for HOA and OOA time series constructed by deconvolution with TSVD and Tikhonov regularization of staggered measurements of length ($\Delta\tau$) 4, 6, and 8 h. $\kappa_m = 20\%$ and $T = 57$ h, meaning each data point is an average over 4 (= 228/57) time series segments. The boundary value methods are full; trunc, truncated; unipad, uniformly padded; and reepad, reflectively padded. The vertical bars represent 95% confidence intervals determined by bootstrapping the mean estimates.

Sampling strategies and post-processing methods for OA measurement

R. L. Modini and
S. Takahama

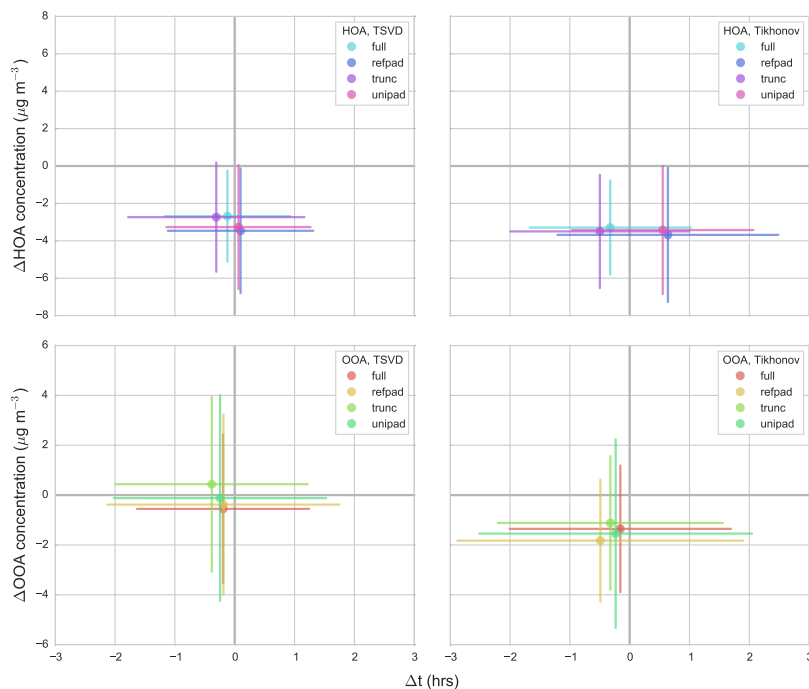


Figure 8. Peak plots for time series of period 57 h measured with 4 h samples subject to 20 % measurement uncertainty recovered by each of the eight combinations of regularization (TSVD, Tikhonov) and boundary value (full, trunc: truncated, unipad: uniformly padded, reypad: reflectively padded) methods. The peak plots are explained fully in the main text in Sect. 4. Briefly, $\Delta[\text{HOA or OOA}]$ concentration represents the mean difference in daily peak concentrations and Δt the mean difference in daily peak timing between a calculated, hourly-resolved time series and its corresponding true time series. The vertical and horizontal bars represent 1 standard deviation of the $\Delta[\text{HOA or OOA}]$ concentration and Δt results, respectively, for each daily peak in all of the modeled solutions.

[Title Page](#)
[Abstract](#)
[Introduction](#)
[Conclusions](#)
[References](#)
[Tables](#)
[Figures](#)
[◀](#)
[▶](#)
[◀](#)
[▶](#)
[Back](#)
[Close](#)
[Full Screen / Esc](#)
[Printer-friendly Version](#)
[Interactive Discussion](#)

Sampling strategies and post-processing methods for OA measurement

R. L. Modini and
S. Takahama

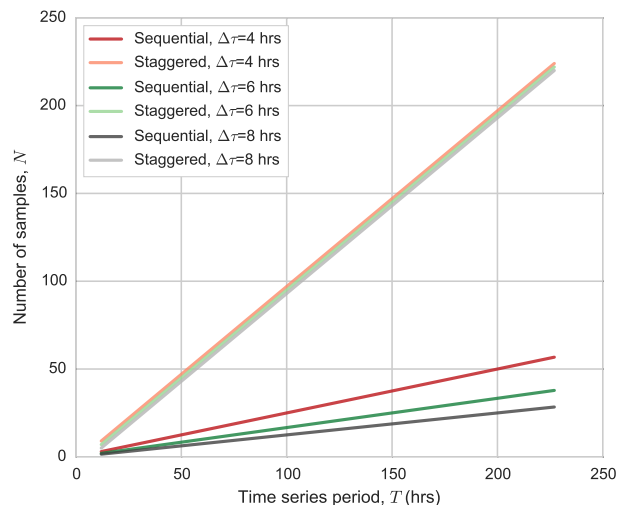


Figure 9. The number of filter samples N of length 4, 6, and 8 h required to measure time series of period T hours sequentially and by staggering the samples at an interval $\delta\tau$ of 1 h. The number of sequential samples is given by $T/\Delta\tau$ and the number of staggered samples is given by $(T - \Delta\tau + 1)/\delta\tau$.

Sampling strategies and post-processing methods for OA measurement

R. L. Modini and
S. Takahama

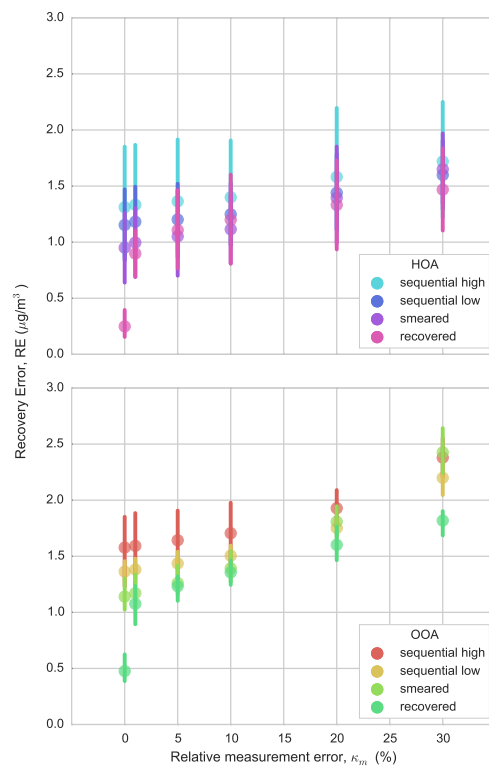


Figure 10. Mean Recovery error (RE) against relative measurement error for HOA and OOA time series processed by the sequential, smeared and recovered methods. $T = 57$ h and $\Delta\tau = 4$ h. The “sequential high” and “sequential low” time series are constructed by linear interpolation between suboptimally- and optimally-scheduled sequential measurements, respectively. The recovered solutions were obtained with TSVD regularization and the truncated boundary method.

[Title Page](#)
[Abstract](#)
[Introduction](#)
[Conclusions](#)
[References](#)
[Tables](#)
[Figures](#)
[◀](#)
[▶](#)
[◀](#)
[▶](#)
[Back](#)
[Close](#)
[Full Screen / Esc](#)
[Printer-friendly Version](#)
[Interactive Discussion](#)

Sampling strategies and post-processing methods for OA measurement

R. L. Modini and
S. Takahama

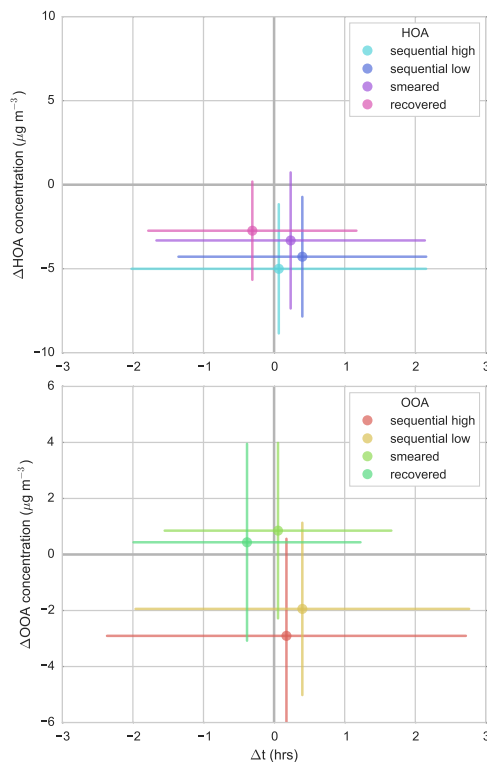


Figure 11. Peak plots for time series of period 57 h measured with 4 h samples subject to 20 % measurement uncertainty processed by the sequential, smeared and recovered methods. The “sequential high” and “sequential low” time series are constructed by linear interpolation between suboptimally- and optimally-scheduled sequential measurements, respectively. The recovered solutions were obtained with TSVD regularization and the truncated boundary method. The peak plots are explained fully in the main text in Sect. 4.

[Title Page](#)[Abstract](#)[Introduction](#)[Conclusions](#)[References](#)[Tables](#)[Figures](#)[◀](#)[▶](#)[◀](#)[▶](#)[Back](#)[Close](#)[Full Screen / Esc](#)[Printer-friendly Version](#)[Interactive Discussion](#)

Sampling strategies and post-processing methods for OA measurement

R. L. Modini and
S. Takahama

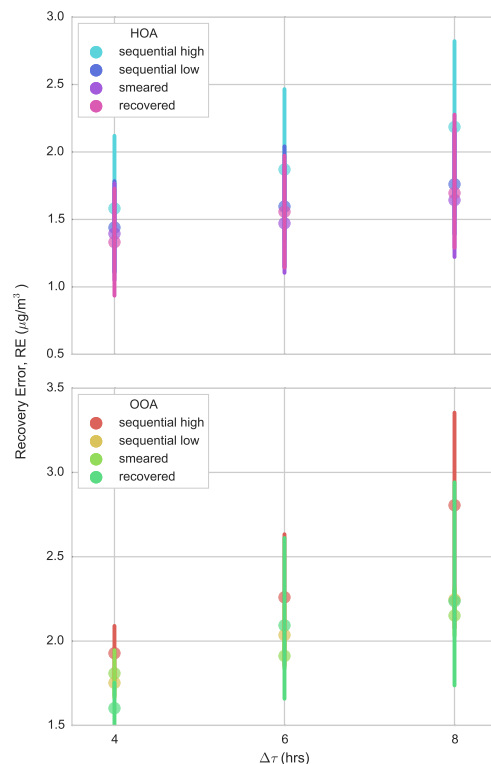


Figure 12. Mean Recovery error (RE) against sample collection time for HOA and OOA time series processed by the sequential, smeared and recovered methods. $T = 57$ h and $\kappa_m = 20$ %. The “sequential high” and “sequential low” time series are constructed by linear interpolation between suboptimally- and optimally-scheduled sequential measurements, respectively. The recovered solutions were obtained with TSVD regularization and the truncated boundary method.

Sampling strategies and post-processing methods for OA measurement

R. L. Modini and
S. Takahama

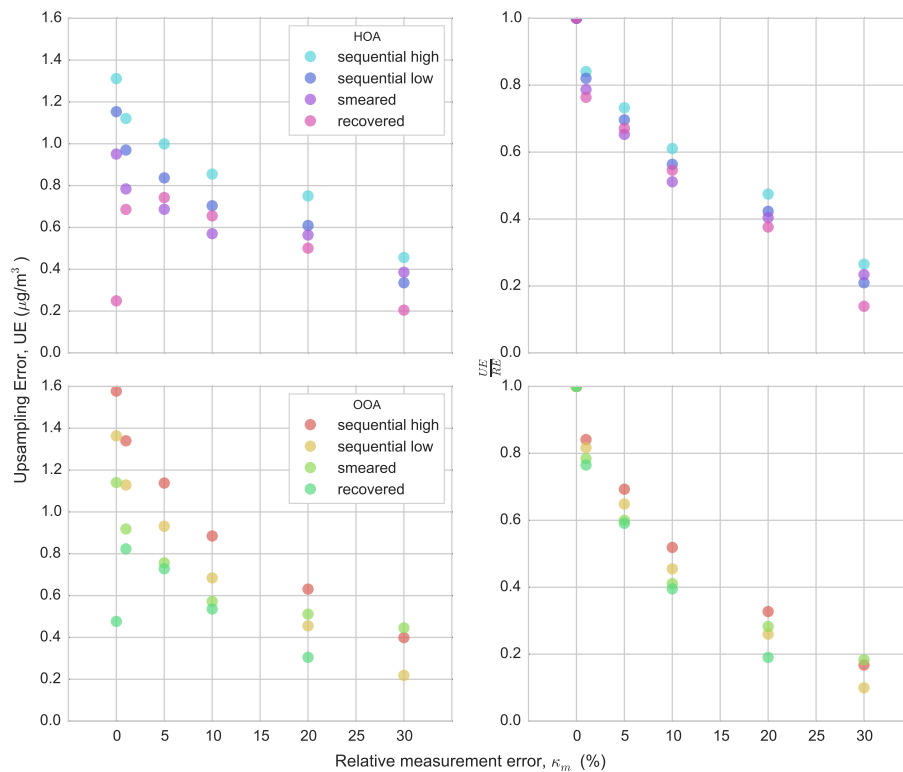


Figure 13. Left panels: upsampling error (UE) vs. κ_m for HOA and OOA time series ($T = 57$ h) measured with 4 h samples. Right panels: the corresponding UE fractions of the total error (RE) as a function of κ_m .